Construction and Building Materials 349 (2022) 128759

Contents lists available at ScienceDirect

Construction and Building Materials

journal homepage: www.elsevier.com/locate/conbuildmat

Rebar corrosion and ASR durability assessment of fly ash concrete mixes using high contents of fine recycled aggregates

Andrés Barragán-Ramos *, Camilo Ríos-Fresneda, Juan Lizarazo-Marriaga, Nicole Hernández-Romero

Universidad Nacional de Colombia, Bogotá, Colombia

ARTICLE INFO

Keywords:
Concrete durability
Recycled concrete aggregate
Durability of concrete
ASR
Steel rebar corrosion

ABSTRACT

This research assessed the potential alkali silica reaction (ASR) of fine recycled aggregates (FRA) derived from precast concrete slabs using petrographic examination and expansion tests, the effects of incorporating FRA on some chloride related transport properties and the corrosion risk of fly ash blended concretes. Mixes incorporating 20 % fly ash (FA) were produced using water-to-binder ratios of 0.45 and 0.50 and FRA replacements of 0 %, 20 %, 60 % and 100 % to test concrete's mechanical performance, chloride penetrability and rebar corrosion risk using electrochemical techniques at different ages. FRA presented an ASR expansion 227 % higher than natural aggregates. Using high contents (>60 %) of FRA didn't increase corrosion risk and a comparable risk to conventional concrete was observed when incorporating FA.

1. Introduction

Construction is responsible for causing considerable environmental impact due to the extraction of natural resources and the associated pollution resulting from their fabrication ang processing activities [1]. Construction also generates large amounts of waste and debris due to the eventual demolition of buildings that have completed their service life. In the USA, 569 million tons of construction and demolition waste (CDW) were generated in 2014, mainly from demolition activities, In China, 30 % – 40 % of total waste consists of CDW, producing around 3000 million tons [2]. In Colombia, CDW correspond to an estimate of 100 thousand tons per day [3].

When CDW is separated and recycled concrete aggregates (RCA) are used, the resulting concrete known as recycled aggregate concrete (RAC) can achieve similar properties than those of conventional concrete. Nevertheless, little acceptance has been observed in the use of fine RCA (FRA) as the durability-related properties could not guarantee an acceptable service life [4]. It has been reported that the replacement of FRA increases water absorption by immersion and capillary action, and reduces both, carbonation and chloride migration resistances [5]; which are directly related to corrosion risk of the steel rebar reinforcement. The negative effects of incorporating RCA in the durability of concrete could be attributed to the high amounts of old adhered mortar (OAM) derived from the parent concrete [6]. OAM consist mainly of fully or partially hydrated cement particles with high porosity paste adhered to natural aggregates, which causes higher water absorption, lower density and lower abrasion resistance than natural aggregates [7]. The presence of OAM in RCA also produces higher porosity in concrete's microstructure that reduce their durability performance [8–10].

Corrosion consists of electrochemical reactions at the surface between metal and an electrolyte solution. In concrete, the solid and liquid products resulting from cement hydration form a thin layer over the rebar surface, known as the passive film, which protects the metal from further corrosion. Regardless of the formation of this film, external ions can be transported through the concrete and in practice, corrosion is never equals to zero but should be kept at very low levels to maintain the service life of reinforced concrete [11]. The stability of metal could be described in terms of its electrochemical potential (EP), which is defined as the ease of ionizing an atom of the metal. EP is dependent on the pH and factors such as the oxygen and water availability. There are ranges of electrochemical potential and pH in which the products of corrosion are either dissolved ions such as Fe^{2+}, solid oxides or hydroxides. The Pourbaix diagram for iron, indicates regions of potential and PH in which the metals will be immune, will actively corrode or will form passive films. Steel bars embedded in concrete are considered to be in a state of passivity due to the high alkalinity of concrete [11].

Abbreviations: RCA, Recycled concrete aggregates; FRA, Fine recycled aggregates; ASR, Alkali silica reaction; FA, Fly ash; OAM, Old attached mortar.

* Corresponding author.
E-mail address: afbarraganr@unal.edu.co (A. Barragán-Ramos).

https://doi.org/10.1016/j.conbuildmat.2022.128759
Received 11 April 2022; Received in revised form 9 July 2022; Accepted 8 August 2022
Available online 17 August 2022

Chloride ions can be present in concrete due to the use of chloride-contaminated components, the use of de-icing salts or from environmental exposure in coastal areas. When the chloride ions in concrete are present in the pore solution, they are called free chlorides and are responsible for initiating the corrosion process [12]. Studies have shown that there is a linear relationship between the chloride penetrability and the increasing replacement of RCA [13]. It has been reported that RAC using 100 % FRA showed a migration coefficient increase of 33.8 % compared to conventional concrete [14]. As the migration coefficient is directly linked to concrete porosity, a reduction of chloride ion penetration resistance is expected when FRA are used [13,15,16].

Alkali-Aggregate reactions are detrimental chemical reactions in concrete that produce internal expansion and premature loss of serviceability. In very aggressive environments with high pH (pH > 12.5), the silica in the reactive mineral phases within the aggregates could react deleteriously with the highly basic alkali hydroxides (K^+, Na^+) dissolved within the micropores in the matrix of hardened concrete [17]. Studies have identified that alkali-aggregate reaction can occur in RCA when the OAM or the original natural aggregates were reactive [18] and it increases for higher replacement ratios of RCA in new concrete [19]. The extent of the reaction depends on the supply of reactants, if the reactant (unstable siliceous phases) had been depleted in the previously affected concrete source (i.e., highly ASR-damaged RCA aggregates), a slower "secondary" expansion is expected in new RAC [19–21]. Due to this effect, researchers have found that RAC with slightly damaged or highly damaged RCA may have a lower number of cracks than conventional concrete [21]. Different behavior has also been observed depending on the size of the reactive recycled particles as the reactants are consumed faster using FRA than coarse recycled aggregates, showing an expansion reduction effect over time[20]. A delay in expansion was also observed using highly damaged FRA and attributed to the residual cement paste with a lower alkali content obstructing the diffusion of alkalis from the new cement paste [20].

It has been established that the use of supplementary cementitious materials (SCM) such as fly ash (FA), silica fume, ground granulated blast furnace slag (GGBFS), or metakaolin, can prevent ASR by reducing the alkali contribution from Portland cement, inducing pozzolanic reactions that produce calcium silicate hydrate (C—S—H) and lowering the pH of the pore solution [22]. Studies have found that the use of FA is effective to mitigate ASR on RCA; however, a higher content may be required compared to conventional concrete due to the additional alkali content provided by the OAM [18,22]. The use of fly ash (FA) can also improve RAC's durability to chloride penetration [23,24], as it can enhance pozzolanic reactions that result in a denser concrete microstructure due to the pozzolanic reaction between FA, Portland cement hydrating products and OAM [10,15]. The use of FA is also notoriously favorable to the increase in RAC's electrical resistivity [25]. Different studies have concluded that the principal negative effect of incorporating FA to RAC is an increase in carbonation depth, as it causes a reduction in concrete's pH due to the pozzolanic reaction between portlandite and FA, which reduces the amount of $Ca(OH)_2$, creating favorable conditions for carbonation to occur [10,15,25–29].

While the effects of incorporating FRA in concrete's durability have been documented, the relationship between possibly expansive aggregates due to ASR and corrosion in steel reinforcement has not been assessed. The objective of this paper was to perform a microscopic characterization of the FRA and evaluate their potential alkali-silica reactivity. RAC mixes were also produced using different FRA contents to identify its effects on concrete's durability, most specifically the properties related to chloride penetration resistance. Additionally, electrochemical measurement techniques were carried out on steel bars embedded into concrete specimens to measure linear polarization resistance (LPR) which is directly correlated to the corrosion rate of steel reinforcement and it's an indicative of the passivation of steel embedded in concrete. This research also aimed to determine the effectivity of incorporating SCM (specifically class-F FA) as a mitigation technique for both ASR in aggregates and corrosion in concrete mixes. This paper contributes to the knowledge on the relationship between aggregate mineral composition, alkali-silica reactivity, concrete durability performance, steel rebar corrosion and potential mitigation techniques by performing an extensive experimental research program. This paper also provides support for further research regarding RAC structural viability from a durability perspective.

2. Experimental program

2.1. Materials

2.1.1. Aggregates

Coarse natural aggregates (CNA) with a maximum size of 12.7 mm and fine natural aggregates (FNA) with a maximum size of 4.76 mm (Sieve No.4) were obtained from a local quarry. These natural aggregates had a fluvial sedimentary origin, regular size, and partially rounded edges. Fine recycled aggregates (FRA) were obtained from a local concrete manufacturer. FRA were derived from prefabricated structural concrete slabs designed to achieve a compressive strength of 35 MPa and mechanically crushed to achieve a maximum size of 4.76 mm. The physical properties measured on both natural and recycled aggregates such as fineness modulus, specific gravity, absorption (ASTM C128) [30], and materials finer than 75 μm (Sieve No. 200) (ASTM C117) [31] are summarized in Table 1.

Regarding particle size distribution, natural aggregates showed a size distribution satisfying the required gradation limits established in ASTM C33 [32]. Due to the homogeneous crushing process, the amount of FRA particles retained on sieves>1 mm was inferior to the recommended on ASTM C33. Particle size distribution for both natural and recycled aggregates are shown on Fig. 1.

2.1.2. Cementitious materials for concrete mixes

Commercially available blended Portland cement (C) type UG – "Uso General" (*General use cement)* according to Colombian regulation NTC 121 [33] was used in the preparation of all concrete mixes. Class F fly ash (FA) meeting the required physical properties defined in ASTM C618 [34] was used as a supplementary cementitious material. The physical properties measured for the binder (cement and fly ash) are shown in Table 2. Both types of cementitious materials are used extensively by local concrete and cement manufacturers.

The chemical oxide analysis performed for FA using X-ray Fluorescence (XRF) is shown in Table 3.

2.1.3. Water reducing admixture

To avoid possible fresh-state performance loss and achieve the target slump value, a high-range water-reducing admixture super-plasticizer (SP) made from polycarboxylates was incorporated on all concrete mixes. The SP composition does not include chlorides to avoid corrosive reactions on reinforced concrete and met the requirements of American standard ASTM C494 [35] for type A water reducing-admixtures and type F high-range water-reducing admixtures.

2.2. Preparation of concrete mixes

Mixes were cast using water/binder (W/B) ratios of 0.45 and 0.50,

Table 1
Physical properties of the aggregates.

Type of Aggregate	Apparent Density (g/cm^3)	Absorption (%)	Fineness Module -	Materials finer than 75 μm (%)
CNA	2,32	4,62	–	–
FNA	2,45	2,09	2,38	5,66
FRA	2,12	9,48	3,25	9,40

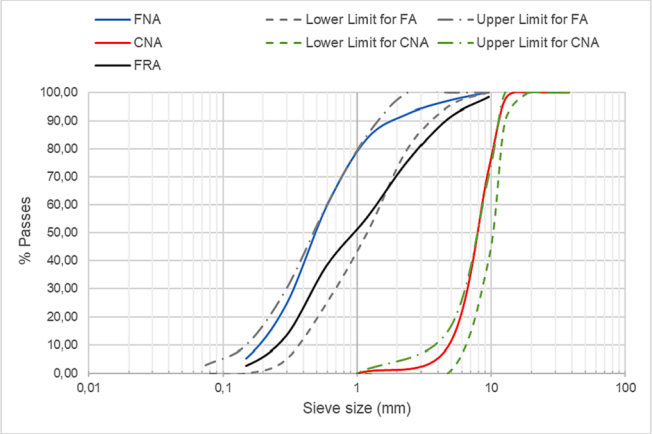

Fig. 1. Grading curves for the aggregates including ASTM C33 limits.

Table 2
Physical properties of used cement and fly ash.

Material	Fineness ASTM C204 (cm^2/g)	Density ASTM C188 (g/cm^3)	Water Content ASTM D7348 (%)	Loss on Ignition (1000 °C) ASTM D7348 (%)
Cement	7014,25	2,82	–	–
Fly Ash	–	2,05	0,41	10,9

Table 3
Chemical composition of fly ash.

	SiO_2 (%)	Al_2O_3 (%)	Fe_2O_3 (%)	CaO (%)	MgO (%)	SO_3 (%)	Na_2O (%)
Fly Ash	55,14	25,33	7,76	1,43	0,78	0,43	0,18

aiming for an average design compressive strength of 21 MPa and 28 MPa as these are the most produced concrete strengths in standard structures. Fourteen mixes were formulated using FRA replacing different contents (0 %, 20 %, 60 % and 100 % by weight) of NFA. Additional six recycled concrete mixes were made replacing 20 % of cement weight by fly ash. The mixture proportions and designations of the different concrete mixes are summarized in Table 4. An optimal volume of 51 % fine and 49 % coarse aggregates that best fits the suggested grading was defined for all FRA contents.

The selected slump for all concrete mixtures was **127 mm ± 25.4 mm (5 ± 1 in.)**. The aggregates were used in air-dry state and the mixing water was compensated to maintain the same effective W/B ratio. SP dosage was defined in the range specified by the manufacturer (0.15 % to 1.2 % of binder weight) and trial mixes were performed with different dosage values until the desired slump was obtained. Each concrete mix was performed following the Two-Stage Mixing Approach (TSMA). This method was proposed by *Tam et al. (2005)*, and different studies have concluded that it may improve recycled aggregate concrete durability and mechanical performance [36–39]. Specimens were demolded after 24 h and cured in moist conditions until testing.

2.3. Test Procedures

2.3.1. Aggregate petrographic testing

Petrographic analysis was carried out following the American standard ASTM C295 [40]. Three thin sections were prepared for each aggregate type. The first one was prepared selecting particles retained on the #8 sieve, the second section was prepared using particles retained on the #16 and #30 sieve, and the third section was prepared using particles retained on the #50 and #100 sieves. The second and third sections were prepared using a different size on each half of the section. A *"Concrete"* lithology was defined for the FRA particles which included fine aggregates, cementing materials and residual clinker and hydration products (OAM). The natural aggregates contained in these particles also included rocks from different lithological origins. The rocks contained in FRA are mostly from sedimentary origin, but igneous and metamorphic origins were also identified.

2.3.2. Alkali-silica reaction in mortar bars

Mortar mixes using Type I ASTM C150 Portland reference cement (OPC), FRA and FNA were formulated to assess the presence of ASR. The procedure and mixing proportions described in ASTM C1260 [41] and ASTM C1567 [42] were followed to produce 25x25x285 mm mortar bars. Three specimens were tested for each mortar mix incorporating different replacement ratios of FRA (0 %, 20 %, 60 %, 80 %, 100 %) and FA (0 %, 20 %). The proportions following ASTM C1260 for each mortar mix are shown on Table 5. The longitudinal expansion of the specimens cured in an aggressive 1 N NaOH solution at 80 °C was measured during a 28-day period.

2.3.3. Hardened concrete

Compressive strength (7, 28 and 90 days) and modulus of elasticity (90 days) were evaluated on cylindrical specimens (100 × 200 mm) according to ASTM C39 [43] and ASTM C469 [44] respectively. Rapid chloride penetration tests (RCPT) (28 and 90 days) were carried out on cylindrical specimens (100 × 50 mm) according to ASTM C1202 [45]. Specimens were also produced to perform water absorption and percent voids tests (28 and 90 days) following the procedure of ASTM C642 [46].

Table 4
Mix proportions of concrete mixes.

Mix	Mix	W/B*	Cement	Fly Ash	Water	Coarse Aggregates	Natural Fine Aggregates	Recycled Fine Aggregates	Super-Plasticizer
			kg/m^3	kg/m^3	kg/m^3	kg/m^3	kg/m^3	kg/m^3	% Binder Mass
1	28-CONTROL	0.45	500	0	225.0	667.7	694.9	0.0	0.32
2	28-RA20	0.45	500	0	225.0	658.6	548.4	137.1	0.35
3	28-RA60	0.45	500	0	225.0	639.7	266.3	399.5	0.35
4	28-RA100	0.45	500	0	225.0	619.8	0.0	645.1	0.35
5	28-RA20-FA20	0.45	400	100	225.0	647.0	538.7	134.7	0.42
6	28-RA60-FA20	0.45	400	100	225.0	628.4	261.6	392.4	0.42
7	28-RA100-FA20	0.45	400	100	225.0	608.8	0.0	633.7	0.42
8	21-CONTROL	0.5	450	0	225.0	688.5	716.6	0.0	0.18
9	21-RA20	0.5	450	0	225.0	679.2	565.5	141.4	0.18
10	21-RA60	0.5	450	0	225.0	659.7	274.7	412.0	0.20
11	21-RA100	0.5	450	0	225.0	639.1	0.0	665.2	0.20
12	21-RA20-FA20	0.5	360	90	225.0	668.7	556.8	139.2	0.25
13	21-RA60-FA20	0.5	360	90	225.0	649.6	270.4	405.6	0.25
14	21-RA100-FA20	0.5	360	90	225.0	629.3	0.0	655.0	0.25

Table 5
Mortar mix proportion for ASR mortar-bar method testing.

Mix ID	Mix Name	Fine Natural Aggregates	Fine Recycled Aggregates	Ordinary Portland Cement	Fly Ash
		g	g	g	g
1	100-NA	990	0	440	0
2	100-RA	0	990	440	0
3	20-RA-20-FA	792	198	352	88
4	60-RA-20-FA	594	594	352	88
5	80-RA-20-FA	198	792	352	88

2.3.4. Electrochemical measurement of corrosion

Corrosion consists of an anodic reaction in which a metal is oxidized end electrons are released, and a cathodic reaction in which the electrons are consumed or reduced. By equating these two reactions, a corrosion current I_{Corr}, which is a direct measurement of the rate of dissolution or oxidation of the metal, and a corrosion potential or open circuit potential, E_{Corr}, can be measured using specialized equipment [11]. The Linear Polarization Resistance (LPR) is the resistance of a specimen to oxidation while an external potential is applied:

$$R_p = \frac{\Delta E}{\Delta I} \tag{1}$$

Where ΔE is the change in electrical potential and ΔI is the change in electrical current. The corrosion current and the corrosion current density (i_{Corr}) can be calculated using the mixed-theory potential developed by Stern and Geary, using the following equations:

$$I_{corr} = \frac{B}{R_p} \tag{2}$$

$$_{icorr} = \frac{B}{R_p A} \tag{3}$$

$$B = \frac{\beta_a \beta_c}{2.3(\beta_a + \beta_c)} \tag{4}$$

A is the surface area of the polarized zone, B is Stern-Geary constant and β_a and β_c are anodic and cathodic Tafel constants, respectively. The Stern-Geary constant should be determined empirically, however, for corrosion of steel rebar in concrete, B is assumed to be equal to 0.026 V for active corrosion and 0.052 V for passive corrosion [11]. The electrical resistance measured by the LPR is the sum of the polarization resistance and the electrolyte resistance R_Ω. For environments such as concrete, R_Ω is significant in magnitude to the total polarization resistance and should be considered and subtracted in the measurements [47]. According to some researchers, corrosion current densities over 1 μA/cm^2 are identified as the level of high corrosion risk and corrosion current densities below are defined as passive corrosion in the system [11]. A corrosion risk classification based on the measured corrosion current density has been formulated [48] as shown on Table 6.

The corrosion current density can be related to the corrosion rate (*CR*) in μm/year by determining the mass loss during the polarization time and applying Faraday's law as following:

$$CR = \frac{i_{corr} * t_a * M_{Fe}}{Z_{Fe} * F * d_{Fe}} * 10^6 \left(\frac{\mu m}{year}\right) \tag{5}$$

Where t_a is the number of seconds in a year (31536000 s/year), M_{Fe} is the molar mass of iron (0.055847 kg/mol), Z_{Fe} is the number of loss electrons (2 for iron), F is Faraday's constant (96485C/mol), and d_{Fe} is the density value for iron (7860 kg/m^3). Therefore, the previous equation can be rewritten as:

$$CR\left(\frac{\mu m}{year}\right) = i_{corr}\left(\frac{A}{cm^2}\right) * 1161 \tag{6}$$

Table 6
Corrosion risk according to corrosion current density. Retrieved from López, Pérez et al. (2006) [48].

Current Density $-i_{corr}$ (μA/cm^2)	Risk of Corrosion
<0.1	Low
0.1–0.5	Moderate
0.5–1	High
>1	Very High

The main advantage of using LPR is that it is a non-destructive method and requires only a few minutes to obtain the corrosion rate; however, since the actual corroding area of steel is hard to determine, an underestimation of the actual corrosion current density is usual [11]. To perform a better estimation of the corroding area, smooth (non-corrugated) steel bars were used. The bars were also painted with epoxy paint to control the exposed area in concrete in which electrode reduction occurs.

Linear Polarization resistance (LPR) measurements were performed using a potentiostat as described in ASTM G59 [49] on 6 mm steel bars embedded on Ø3-inch cylindrical specimens from the same concrete mixes submerged in a 3 % NaCl solution as shown in Fig. 2 (a). Initial LPR was measured for three specimens of each concrete mix after 28 days of moist curing conditions in 20 °C tap water. Following the initial LPR tests, specimens were submerged in a 3 % NaCl solution and tested after 1, 2 and 3 months of chloride solution immersion. A three-point electrode system shown in Fig. 2 (b) was used for LPR measurements. The working electrode was defined as the specimen under testing, in this case the embedded steel bars. The counter electrode was a graphite bar that completed the current path. The used reference electrode was a saturated calomel electrode (SCE). Experiments were performed at a voltage scan rate of 0.36 V/h (0.1 mV/s) from a potential of −30 mV to 30 mV. Since LPR tests measure the total specimen electrical resistance (concrete plus steel bar) and corrosion density calculation requires the resistance value of only the embedded steel, Electrochemical Impedance Spectroscopy (EIS) tests were also performed to measure the medium (concrete) electrical resistance.

3. Results and discussion

3.1. Aggregate petrographic testing

The content of each predominant lithology for the employed aggregates are summarized on Table 7. It is possible to identify that the main difference between natural and recycled aggregates is the presence of a "concrete" aggregate type which contains aggregates with old-attached mortar (OAM) and cement or hydration products in smaller particle sizes. Sedimentary rocks without OAM such as chert were also identified for the larger FRA sizes. For the aggregates retained on the #100 sieve, the "concrete" aggregate type was no longer identified and both FRA and FNA had a similar composition with a high presence of feldspar and plagioclase. A high content of straight and high strained quartz was observed for both types of aggregates due to the predominant sedimentary origin of the aggregates.

The mineral origin of the FNA was more heterogeneous, having a significant content of metamorphic and igneous aggregates. Since the natural aggregates had a fluvial origin, particles are usually transported many kilometers before being deposited, which results in a wide variety of minerals with diverse origins. The larger sizes of FRA also showed combinations of sedimentary, igneous, and metamorphic aggregates bonded to hydration products from the parent concrete as shown in Fig. 3. Both types of aggregates had low porosity and non-homogeneous shapes and minor levels of carbonation were observed on FRA. For FRA

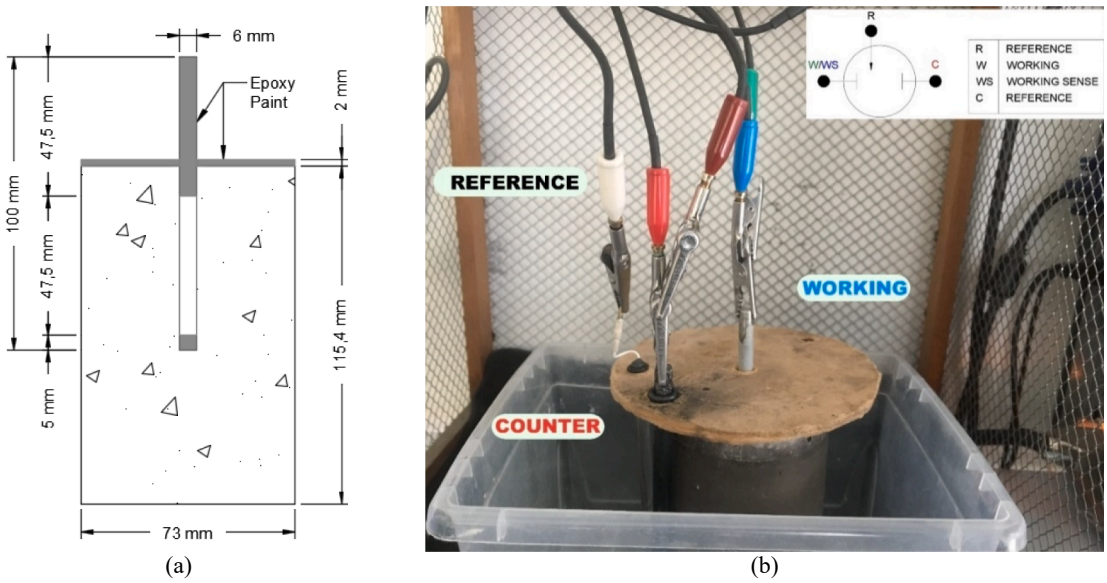

Fig. 2. (a) Cylindrical specimens with embedded steel bar. (b) Three-point electrode system used for PR tests.

Table 7
Predominant lithologies for each aggregate size.

Sieve Size	Fine Recycled Aggregates		Fine Natural Aggregates		Coarse Natural Aggregates	
	Lithologies	%	Lithologies	%	Lithologies	%
#8 (2.38 mm)	Concrete	64.9	Chert	20.7	Quartz Sandstone	66.7
	Chert	20.5	Diorite	16.7	Silicate Mudstone	12.0
	Silicate Siltstone	6.6	Quartz Sandstone	8.7	Chert	10.7
	-	-	Silicate Siltstone	9.3	-	-
#16 (1.19 mm)	Concrete	61.2	Chert	17.3		
	Chert	11.2	Quartz Sandstone	11.3		
	Silicate Siltstone	8.6	Plagioclase	11.3		
	-	-	Quartz Shale	9.3		
#30 (595 μm)	Concrete	67.1	Straight Quartz	22.0		
	Chert	10.7	High strained Quartz	13.3		
	Quartz	5.3	Plagioclase	16.0		
#50 (297 μm)	Concrete	43.3	Straight Quartz	19.3		
	Straight Quartz	10.7	High strained Quartz	16.0		
	Feldspar	12.7	Feldspar	15.3		
#100 (149 μm)	Straight Quartz	48.7	Straight Quartz	16.0		
	Plagioclase	17.3	Plagioclase	20.7		
	Feldspar	10.7	Feldspar	15.3		
			Hornblende	14.7		

particles, no signs of previous ASR related expansion or cracking was identified.

Regarding alkali-silica reaction (ASR), multiple potentially alkali-silica reactive lithologies such as chert, quartzites and phyllites were identified. The main identified reactive components of these lithologies are summarized for each particle size in Table 8. For both types of fine aggregates, the main reactive mineral in the particles was high strained quartz observed in metamorphic aggregates (29.6 % in FRA and 21 % in FNA) followed by microcrystalline quartz which was present in the sedimentary rocks like chert and mudstone (16.1 % in FRA and 15.5 % in FNA). FRA showed approximately 10 % higher content of potentially reactive minerals. In average, a potentially reactive component was identified for 45.7 % of all FRA particles and 36.8 % of all FNA particles.

Based only on the mineral composition of the aggregates (excluding the possible reactive effects of OAM), for this research program the concrete mixes made with both types of aggregates could be similarly reactive depending on the cementing material used. Apart from the hydration products on the "concrete" lithology from FRA, no significant difference was observed on the mineral composition of the aggregates. It is important to notice that the petrographic analysis was used to identify the lithology, origin and reactive minerals of the natural aggregates and the original aggregate portion of FRA (excluding OAM). For FRA, it was possible to assess the existence of hydration products from a "concrete" lithology but due to the chemical composition of this cementitious matrix, the potentially reactive alkaline ions cannot be identified using petrographic analysis and further assessment using ASTM C1260 [41] and ASTM C1567 [42] was formulated.

3.2. Alkali-silica reaction of mortar bars

According to ASTM standards, mortar bars cast using potentially expansive aggregates will have an expansion>0.10 % after 16 days of a hot and alkaline curing. The obtained bar expansion for each mix is plotted against the specimen age in Fig. 4. Results showed that the used FRA are potentially expansive, having an expansion of approximately 0.25 % at 16 days. The used NFA showed an expansion of approximately 0.11 % at 16 days, staying slightly above the defined limit. These results are consistent with other researchers who have reported that alkali-aggregate reaction can occur when the OAM or the original natural aggregates were reactive [18] and increases for higher replacement ratios of FRA [19].

Petrographic analysis revealed a very similar mineral composition between FNA and FRA, this would indicate that the high alkalinity content of the OAM is responsible for the observed expansion. Previous studies have also reported that FRA derived from previously ASR-damaged concrete showed lower expansion than FRA derived from non-damaged parent concrete as the alkali supply is higher [19–21]. This is consistent with the obtained results as the petrographic examination revealed no previous cracking or expansion in the OAM or aggregates related to ASR, suggesting that the OAM of the employed FRA supplied a high number of free alkalis that had not been consumed previously. It has also been reported that the reactants are consumed

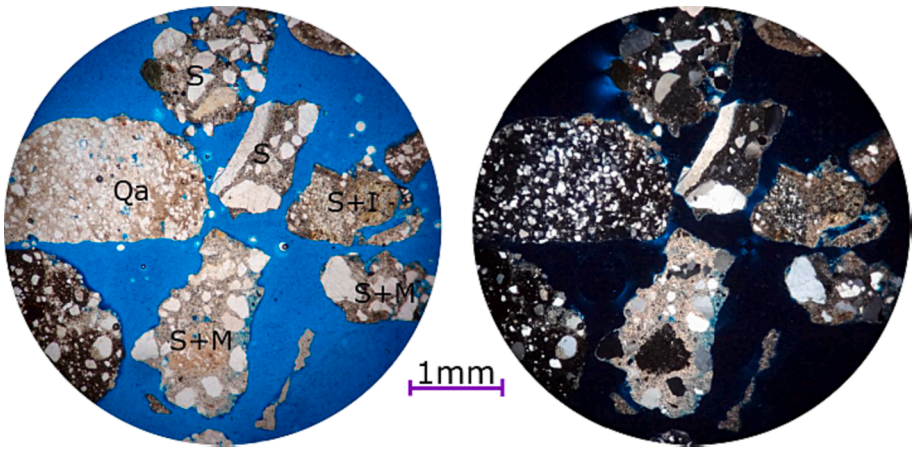

Fig. 3. PPL - XPL Microphotography of RCA with Quartz Sandstone (Qa), cement with sedimentary and metamorphic aggregates (S + M), Cement with Sedimentary and Igneous aggregates (S + I). and Cement with Sedimentary aggregates (S).

Table 8
Potentially reactive components identified in FNA and FRA.

Reactive components content (%)	Fine Recycled Aggregates						Fine Natural Aggregates					
Sieve Size	#8	#16	#30	#50	#100	Avg	#8	#16	#30	#50	#100	Avg.
Mycrocristalline Quartz	27.3	21.3	16.0	13.3	2.7	16.1	32.7	24.7	8.7	8.0	3.4	15.5
Highly Strained Quartz	48.7	37.3	38.7	16.0	7.4	29.6	26.0	20.7	24.0	18.0	16.1	21.0
Total	76.0	58.7	54.7	29.3	10.1	45.7	58.7	45.4	32.7	26.0	19.5	36.5

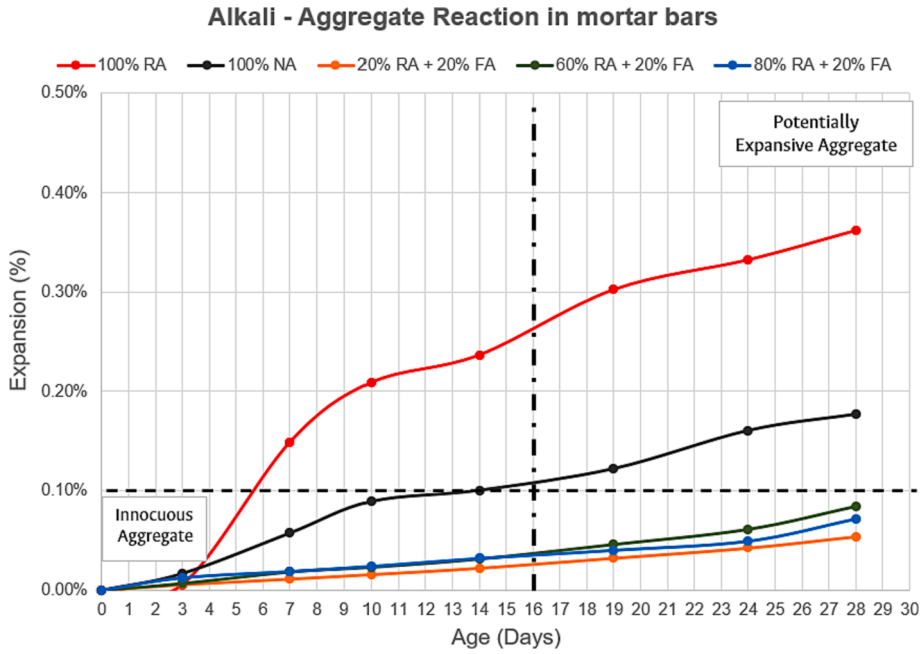

Fig. 4. Expansion of mortar bars for different mortar mixes.

faster using FRA, showing an expansion reduction effect over time [20]; however, this reduction in the expansion rate was not observed and the mortar mix containing 100 % FRA showed the same expansion rate even after 28 days of curing in a very aggressive environment. This may be attributed to the initial alkali content of the aggregates and the achieved particle suspension of fine aggregates inside the cement matrix, which may allow a higher reactant interchange. Results indicate that the ASR observed on mixes with FRA does not depend only on the mineral composition of the aggregates, but it is also highly affected by the alkali supply of the OAM. Mortar bar expansion methods may also be more effective to detect potential ASR reactivity since the alkali content of OAM cannot be identified only by petrographic/microscopic examination.

Results from the mortar bars including fly ash, revealed an innocuous expansive behavior even when employing 80 % replacement of FRA. This would indicate that FA is a very effective pozzolan for reducing expansive negative reactions when using FRA. This has been observed by other researchers who claimed that fly ash reduces the alkalinity of recycled aggregates and neutralizes possible chemical reactions that result in bar expansion by reducing the pH of the fluids saturating the